

# Why Seasonal Prediction of California Winter Precipitation Is Challenging

Xianan Jiang , Duane E. Waliser, Peter B. Gibson, Gang Chen, and Weina Guan

**ABSTRACT:** Despite an urgent demand for reliable seasonal prediction of precipitation in California (CA) due to the recent recurrent and severe drought conditions, our predictive skill for CA winter precipitation remains limited. October hindcasts by the coupled dynamical models typically show a correlation skill of about 0.3 for CA winter (November–March) precipitation. In this study, an attempt is made to understand the underlying processes that limit seasonal prediction skill for CA winter precipitation. It is found that only about 25% of interannual variability of CA winter precipitation can be attributed to influences by El Niño–Southern Oscillation (ENSO). Instead, the year-to-year CA winter precipitation variability is primarily due to circulation anomalies independent from ENSO, featuring a circulation center over the west coast United States as a portion of a short Rossby wave train pattern over the North Pacific. Analyses suggest that dynamical models show nearly no skill in predicting these ENSO-independent circulation anomalies, thus leading to limited predictive skill for CA winter precipitation. Low predictability of these ENSO-independent circulation anomalies is further demonstrated by a large ensemble of atmospheric-only climate model simulations. While low predictability of the ENSO-independent circulation anomalies could be due to chaotic internal atmospheric processes over the mid- to high latitudes, possible underexploited predictability sources for CA precipitation in models are also discussed. This study pinpoints an urgent need for improved understanding of the formation mechanisms of ENSO-independent circulation anomalies over the U.S. West Coast for a breakthrough in seasonal prediction of CA winter precipitation.

**KEYWORDS:** Extratropical cyclones; Drought; Climate prediction; Seasonal forecasting; Climate variability

<https://doi.org/10.1175/BAMS-D-21-0252.1>

Corresponding author: Dr. Xianan Jiang, [xianan@ucla.edu](mailto:xianan@ucla.edu).

Supplemental material: <https://doi.org/10.1175/BAMS-D-21-0252.2>

In final form 15 September 2022

©2022 American Meteorological Society

For information regarding reuse of this content and general copyright information, consult the [AMS Copyright Policy](#).

**AFFILIATIONS:** **Jiang**—Joint Institute for Regional Earth System Science and Engineering, University of California, Los Angeles, Los Angeles, and Jet Propulsion Laboratory, California Institute of Technology, Pasadena, California; **Waliser**—Jet Propulsion Laboratory, California Institute of Technology, Pasadena, California; **Gibson**—National Institute of Water and Atmospheric Research, Wellington, New Zealand; **Chen**—Department of Atmospheric and Oceanic Sciences, University of California, Los Angeles, Los Angeles, California; **Guan**—Joint Institute for Regional Earth System Science and Engineering, University of California, Los Angeles, Los Angeles, California, and Center for Monsoon System Research, Institute of Atmospheric Physics, Chinese Academy of Sciences, Beijing, China

**E**xtrême climate variability poses a serious threat to California (CA), the nation’s most populous state and one that plays a crucial role in U.S. economy, including from agriculture and food supplies. Following a long-lasting statewide drought in CA during 2012–16, severe dry and warm conditions reemerged in CA since 2019 and are still developing at the time of writing. The years 2020 and 2021 were marked as the fifth and second driest years in CA during the past 100 years, respectively, while January–March 2022 were identified as the months with least rain and snow in CA.<sup>1</sup> Due to significant risks posed by these multiyear droughts to local water supply and management, agriculture production, and wildfire severity and frequency, etc., a drought state of emergency has been declared in CA since 2021.

<sup>1</sup> <https://drought.ca.gov/current-drought-conditions/>

Considering the great challenges presented by these climate extremes, accurate prediction of CA precipitation several months ahead becomes particularly important for disaster preparation and mitigation as well as for drought and water restriction policy-making purposes (DeFlorio et al. 2021; Sengupta et al. 2022). Precipitation over CA largely occurs during its winter season with maxima over mountainous areas in the form of snowpack (Fig. 1a), often associated with landfalling atmospheric rivers (Dettinger 2011; Waliser and Guan 2017; Ralph et al. 2017). Due to its location over a transition region between two climate regimes that are associated with midlatitude storms and the subtropical high, CA winter precipitation exhibits pronounced year-to-year variability (Fig. 1b). Previous studies have indicated considerable difficulty in skillfully predicting CA winter precipitation (e.g., Seager et al. 2015; Wang et al. 2017; Gibson et al. 2020a,b; Kumar and Chen 2020), with typical correlation skill of 0.1–0.4 for seasonal prediction of CA winter precipitation in our latest prediction systems (Gibson et al. 2021; Kumar and Chen 2020).

The anomalous sea surface temperature (SST) condition over the Pacific, e.g., El Niño, has been considered a primary predictor for seasonal prediction of CA precipitation, with wet (dry) conditions in CA during El Niño (La Niña) winters (Schonher and Nicholson 1989; Barnston and Smith 1996; Trenberth et al. 1998; L’Heureux et al. 2015; Jong et al. 2016; Seager et al. 2010; Gibson et al. 2021). While a statistically significant correlation of about 0.5 between CA precipitation and the El Niño index during the past four decades is observed (Fig. 1b), it suggests that less than 25% of the year-to-year variability of CA precipitation can be explained by El Niño–Southern Oscillation (ENSO).<sup>2</sup> This notion is largely in agreement with previous studies (e.g., Cash and Burls 2019; Kumar and Chen 2020). Therefore, tropical SST condition alone may not be sufficient for skillful or useful prediction of winter

<sup>2</sup> This estimate is based on the Niño-1+2 index as shown in Fig. 1b, which exhibits a higher correlation with CA winter precipitation than other El Niño indices, including the Niño-3.4 index and the ENSO longitude index (see supporting Fig. S1 and to be further discussed in Fig. 3a).

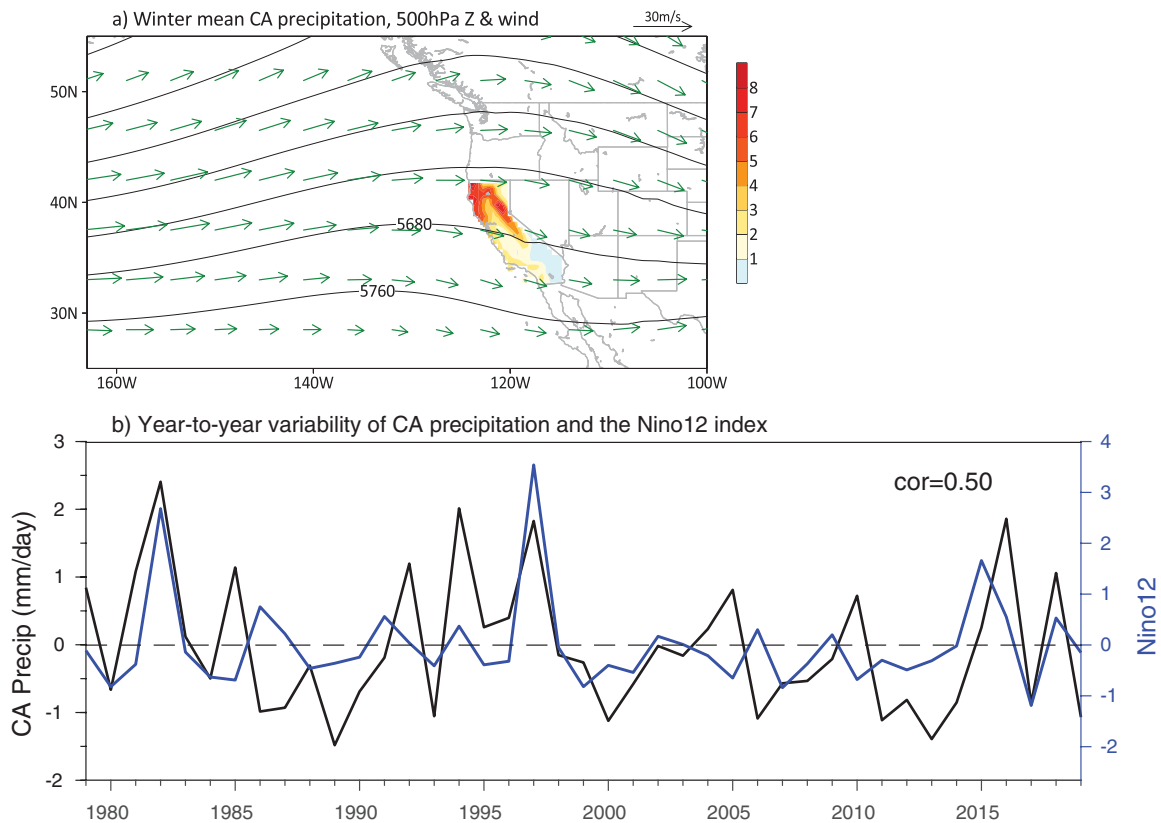


**Fig. 1.** (a) Climatological winter (November–March) mean precipitation over California (shading; mm day<sup>-1</sup>), geopotential height ( $Z$ ; gpm) and winds (see the vector scale on the upper right) at 500 hPa. (b) The year-to-year variability of CA winter precipitation anomalies (black) along with the Pacific Niño-1+2 index (blue; K). The Pearson correlation coefficient between these indices is also shown.

CA precipitation (e.g., Seager et al. 2015; Hoell et al. 2016; Cash and Burls 2019; Wang et al. 2017; Kumar and Chen 2020). One good example is the failure in predicting CA precipitation during the period of 2012–16 drought (L’Heureux et al. 2021). Given the presence of a major El Niño event in 2015/16, increased winter precipitation over CA was highly anticipated to break the long-lasting drought, but the 2015/16 winter turned out to be another dry year in most areas of CA. In contrast, an unexpectedly significant amount of precipitation in CA occurred in the 2016/17 winter despite a weak La Niña condition. As shown in Fig. 1b, while several extreme wet winters over CA are linked to major El Niño events during the past four decades, e.g., 1982/83, and 1997/98 winters, El Niño (La Niña) conditions are not closely associated with other majority of extreme wet (dry) conditions over CA.

The somewhat limited predictive skill of CA precipitation based on ENSO is partially due to challenges in predicting the ENSO-induced teleconnection patterns (e.g., Bayr et al. 2019; Kumar and Chen 2020), but can also be attributed to other factors that contribute to the variability of CA precipitation, including internal variability of circulation anomalies in the midlatitudes (Baxter and Nigam 2015; Chen and Kumar 2018; Swenson et al. 2019; Kumar and Chen 2020; Gibson et al. 2021), SST anomalies and induced diabatic heating over the western Pacific, Indian Ocean, or extratropical North Pacific (Wang et al. 2014; Seager et al. 2015; Hartmann 2015; Lee et al. 2015; Yang et al. 2018; Gibson et al. 2020b), or possibly Arctic sea ice variability (Cohen et al. 2017). While most of these previous studies in exploring predictors for CA precipitation were based on case studies, it remains elusive how predictable the year-to-year variability of CA winter precipitation is and why it is challenging to achieve skillful seasonal prediction of CA precipitation.

In this study, we analyze long-term hindcasts from multiple atmosphere–ocean coupled models participated in the North American Multimodel Ensemble (NMME) Project

(Kirtman et al. 2014; Becker et al. 2014, 2022), as well as simulations from a series of large-ensemble atmospheric-only global climate models (AGCMs), to address the following questions: What are the key anomalous circulation patterns affecting winter CA precipitation beyond the influences of ENSO? How predictable are the ENSO-independent circulation patterns associated with interannual CA precipitation? Answers to these questions will provide insights to inform future investigations toward improved prediction of CA winter precipitation.

### **Observational datasets**

The observed monthly mean precipitation used in this study are obtained from two datasets: the high resolution (0.5°) NOAA Climate Prediction Center (CPC) unified gauge-based precipitation dataset (Chen et al. 2008) is used to derive precipitation over the CA region (spatial average over total 183 0.5° grid points within the CA state), and the 1° precipitation data from the Global Precipitation Climatology Project (GPCP; version 2, revision 3; Adler et al. 2003) are used to derive global precipitation patterns associated with CA precipitation. The observed El Niño indices (Niño-1+2 and Niño-3.4) were obtained from the NOAA Physical Science Laboratory website. The observed SST used for this study is from the Met Office Hadley Centre (Rayner et al. 2003). The latest ERA5 reanalysis from ECMWF (Hersbach et al. 2020) is used to characterize large-scale patterns associated with CA precipitation. All observational datasets analyzed in this study are from 1979 to 2019. The winter season is defined by November–March with anomalies for each winter calculated by departures from the 1979–2019 climatology.

### **Predictive skill of CA winter precipitation in NMME hindcasts**

We first illustrate how well CA winter precipitation is predicted in the state-of-the-art dynamical coupled models participated in the NMME Project (Kirtman et al. 2014; Becker et al. 2014). Predicted ensemble mean winter precipitation anomalies over CA from hindcasts issued on October 1 of each year by three NMME models (CESM1, GEOS5, and FLORB) are illustrated along with each member prediction and the observations in Fig. 2. Note that precipitation anomalies in model predictions are defined by departures from each model's climatology. Consistent with previous discussions, all three NMME models show rather limited skill in predicting CA winter precipitation, with a Pearson correlation skill score of ~0.3 during the ~30-yr period based on ensemble mean predictions. Significant deviations among predictions from ensemble members are evident in all three models. Note that while the enhanced CA winter precipitation during 1997/98 El Niño is more or less predicted in all these three models, enhanced CA precipitation during 1982/83 winter is only captured in CESM1 with a reduced amplitude. Low predictive skill of CA precipitation with correlation scores from 0.1 to 0.4 is also noted in other NMME models as reported in Kumar and Chen (2020), in which they also showed a large model spread in predicted CA precipitation associated with El Niño. The low prediction skill for CA precipitation in these NMME models could be due to model biases in predicting the evolution of global SST/sea ice anomalies after initialization, thus their remote influences on CA precipitation, or due to model inability in depicting other key processes associated with CA precipitation that cannot explained by SST/sea ice boundary forcing.

### **Circulation pattern associated with CA precipitation beyond ENSO influences**

As previously discussed in Fig. 1, ENSO can only explain about 25% of the interannual variability of CA precipitation. In this section, to better understand predictability of CA precipitation, we will characterize anomalous circulation patterns associated with CA precipitation that are independent from ENSO.

The observed anomalous global precipitation and circulation at 500 hPa associated with enhanced CA winter precipitation are illustrated in Fig. 3a based on a regression analysis.

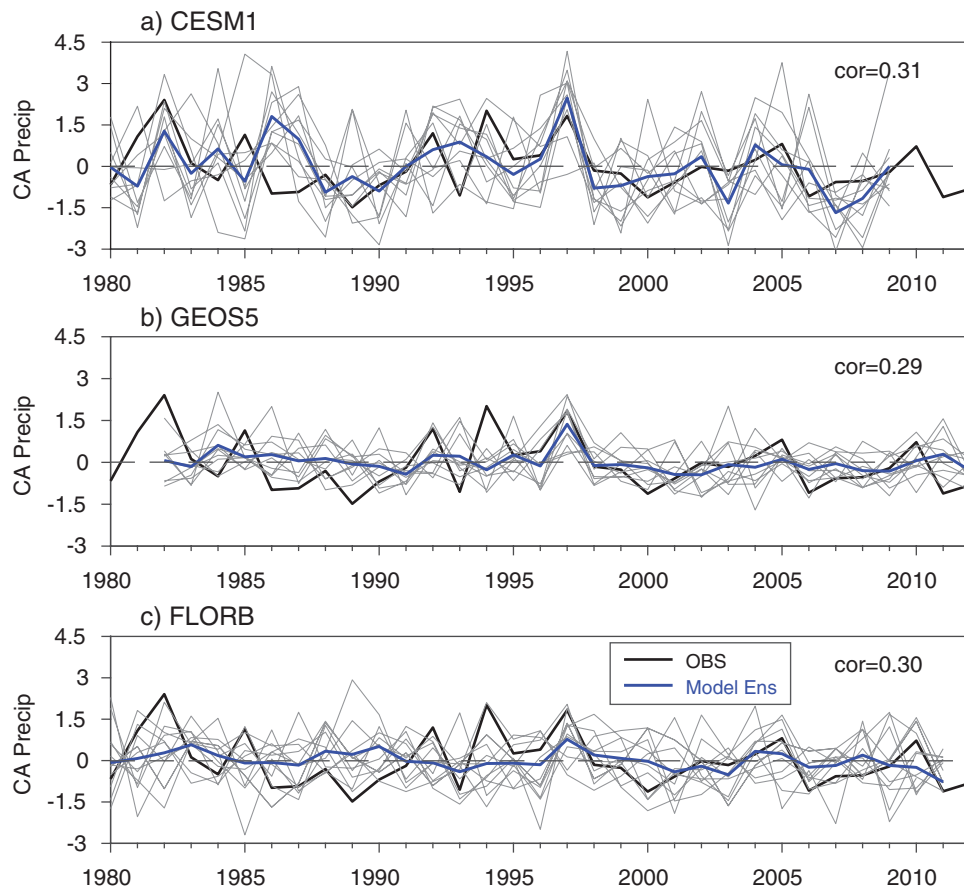


**Fig. 2.** The observed (black) and predicted CA winter precipitation anomalies (blue for ensemble mean predictions and gray for each member prediction;  $\text{mm day}^{-1}$ ) based on three NMME models: (a) CESM1, (b) GEOS5, and (c) FLORB. All these predictions are initialized on 1 October of each year.

Enhanced CA precipitation is accompanied with a relatively broad wet condition over the southwest United States and the neighboring Pacific Ocean along with a weak dry condition to the north along the Pacific coast. This north–south precipitation dipole pattern along west coast of North America (NA) is coupled with an anomalous low pressure system between the two anomalous precipitation centers. The enhanced precipitation over CA tends to be promoted by moisture transport and possibly enhanced atmospheric river activity due to strengthening of the westerly jet stream in the southern part of the anomalous Pacific low. In the tropics, enhanced precipitation is evident over the central and eastern Pacific while suppressed convection over the western Pacific and the southern Pacific convergence zone (SPCZ). These characters are reminiscent of the ENSO impacts on CA precipitation, which is confirmed by strong positive correlations between eastern Pacific SST anomalies and CA precipitation (purple contours in Fig. 3a). The maximum correlations are found over the far eastern Pacific over the coastal region off South America, i.e., the Niño-1+2 region, in agreement with results previously discussed in Fig. 1b (also see online supporting Fig. S1; <https://doi.org/10.1175/BAMS-D-21-0252.2>). Therefore, in the following we will use the Niño-1+2 index to represent the ENSO variability instead of the Niño-3.4 index and the ENSO longitude index (ELI) (Williams and Patricola 2018).

Since the anomalous circulation patterns associated with CA precipitation in Fig. 3a can include both influences by ENSO and components that are independent from ENSO, we then attempt to extract ENSO-related Z500 and precipitation anomalies from the total anomalous fields. The ENSO-related Z500 and precipitation anomalies during a particular winter are defined by their respective linear regression patterns against the Niño-1+2 index and normalized by the amplitude of the Niño-1+2 index during that winter. The reconstructed ENSO-related

Z500 and precipitation for the period of 1979–2019 can then be similarly regressed onto CA precipitation to obtain the ENSO-related Z500 and precipitation anomalies associated with CA precipitation variability (Fig. 3b); meanwhile, the anomalies that are independent from ENSO can be obtained by subtracting the ENSO-related components from the total (Fig. 3c).

By definition, the ENSO-related precipitation and circulation anomalies associated with CA precipitation are characterized by typical ENSO signals, with enhanced (suppressed) precipitation over the central/eastern (western) equatorial Pacific, and a slightly shifted Pacific–NA teleconnection pattern over the midlatitudes (Fig. 3b). After removal of the ENSO components, the Z500 anomalous pattern associated with CA precipitation is featured by a short Rossby wave train spanning over the North Pacific basin with a relatively small-scale low pressure system which more directly straddles the west coast of NA (Fig. 3c). Similar local circulation anomalies near the Pacific coast of NA associated with CA precipitation were also previously reported (e.g., Guirguis et al. 2020; Chen et al. 2021). This ENSO-independent anomalous Z pattern over the North Pacific tends to exhibit weak enhanced (suppressed) precipitation over the western (central) equatorial Pacific (Fig. 3c). Similar anomalous circulation and tropical convection patterns as in Fig. 3c were also mentioned in previous studies in association with CA precipitation on subseasonal time scales (e.g., Teng and Branstator 2017; Gibson et al. 2020b). Particularly noteworthy is the dominance of the total CA precipitation in Fig. 3a by the ENSO-independent component (Fig. 3c), with a weak contribution from ENSO (Fig. 3b). Very similar results can be obtained if the ELI index is used to extract the ENSO signals (supporting Fig. S2), indicating that these results are robust to the particular choice of index used.

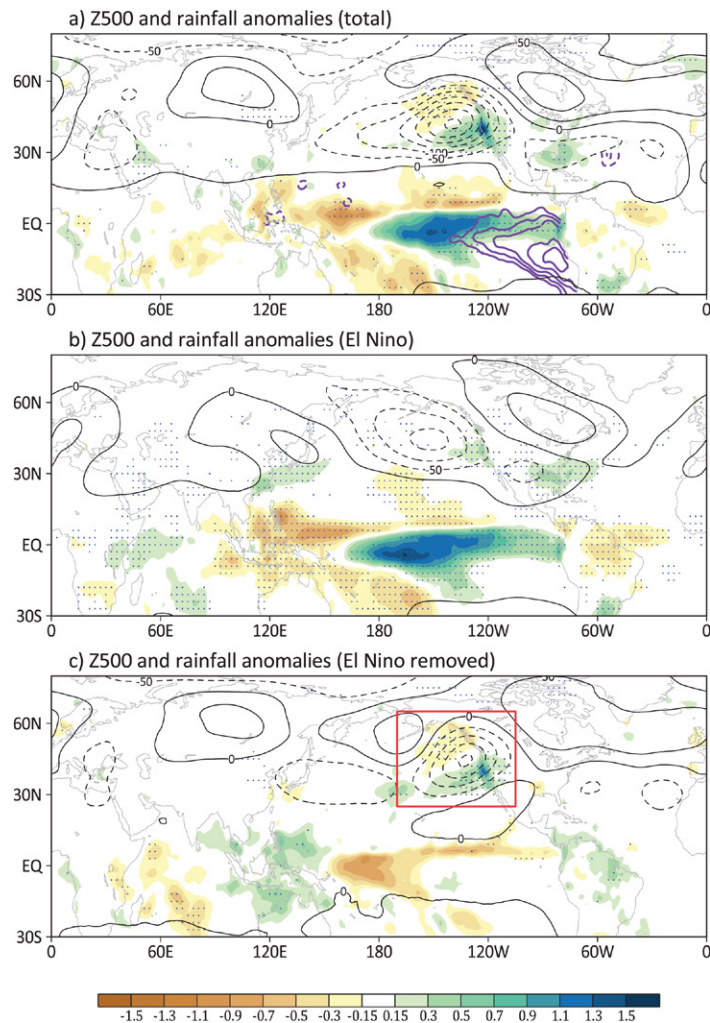


**Fig. 3. Anomalous geopotential height at 500 hPa (Z500; contours; gpm) and precipitation (shaded; mm day<sup>-1</sup>) associated with CA winter precipitation: (a) total anomalies, (b) anomalies associated with the ENSO variability, and (c) anomalies with ENSO signals removed. Purple contours in (a) represent correlations of winter SST anomalies (only shown over 30°S–30°N) against CA precipitation (solid lines for positive correlations and dashed lines for negative correlations with the first contour for  $\pm 0.35$  and an interval of 0.05). Stippled areas represent rainfall anomalies surpassing 95% significance level based on the Student's *t* test of their corresponding correlation coefficients. All these results are based on observations. The observed ENSO-independent anomalous Z pattern over the red box region in (c) is used to define the Pacific\_Z500ne index. See text for more details.**

## Role of ENSO and ENSO-independent circulation anomalies for CA precipitation

To reveal underlying processes responsible for limited skill in predicting CA precipitation, we assess the relative role of ENSO-related and ENSO-independent circulation anomalies over the west coast of North America for CA precipitation prediction using a multilinear regression model. As previously discussed, the ENSO-related circulation pattern can be represented by the Niño-1+2 index based on the regression approach. We then define a Pacific\_Z500ne index (with “ne” denoting the non-ENSO component) to depict circulation anomalies that are independent from ENSO. The observed Pacific\_Z500ne index is derived by projecting anomalous winter mean Z500 pattern based on ERA5, after removal of the ENSO-related signals, onto the Z500 pattern over the Pacific coast of NA associated with CA precipitation (the red rectangular region in Fig. 3c).

We next examine how well CA winter precipitation can be “predicted” by assuming that both the winter Niño-1+2 and Pacific\_Z500ne indices (i.e., both circulation anomalies over the west coast of NA that are induced by or independent from ENSO) can be perfectly predicted. The prediction model is constructed using the linear regression approach with the observed winter Niño-1+2 and Pacific\_Z500ne indices as two predictors,

$$\text{CA\_Precip} = \alpha \times \text{Niño-1+2} + \beta \times \text{Pacific\_Z500ne}, \quad (1)$$

where the two coefficients,  $\alpha$  and  $\beta$ , are derived based on observations for the period of 1979–2019 with cross validations in which factors during the year to be predicted are excluded when deriving the two regression coefficients. Additional experiments can also be conducted to examine how CA precipitation can be predicted by only using the Niño-1+2 or Pacific\_Z500ne index.

As shown in Fig. 4, when only the observed winter Niño-1+2 index is used, the predicted CA precipitation shows a correlation of 0.56 with the observations (Fig. 4a), largely consistent with results previously discussed in Fig. 1b. Higher correlation skill (0.68) is obtained when the Pacific\_Z500ne is used for prediction (Fig. 4b), which captures many drought events after 1986 that are largely missed in prediction by the Niño-1+2 index. When both the Niño-1+2 and Pacific\_Z500ne indices are used, prediction is significantly improved with a correlation skill of about 0.83 (Fig. 4c). This result suggests that if we could eventually accurately predict the winter El Niño condition and the Pacific\_Z500ne index, we would have a much improved chance at skillfully predicting CA precipitation, with these combined indices explaining ~70% of the precipitation variability. For practical seasonal prediction of CA precipitation, the key question then concerns the predictability of the winter Niño-1+2 and Pacific\_Z500ne indices several months ahead, which will be examined in the following by analyzing hindcasts from the NMME models.

## Limiting factors for CA precipitation predictability

Figure 5 presents predicted time series of the winter Niño-1+2 and Pacific\_Z500ne indices based on CESM1, showing both ensemble mean prediction (blue) and prediction from individual members (gray). It is clearly seen that the winter Niño-1+2 index can be very well predicted with a skill of 0.78 between the ensemble mean prediction and observations, and with great consistency among individual members (Fig. 5a). Generally skillful prediction of winter El Niño condition by NMME models when initialized in fall has also been reported (Zhang et al. 2017; L’Heureux et al. 2020; Kumar and Chen 2020). However, the ensemble mean prediction of the Pacific\_Z500ne index in CESM1 shows nearly no correlation with the observations with a significant spread among individual member predictions (Fig. 5b). Based on discussions for Fig. 4, the rather limited skill in predicting CA precipitation is therefore primarily due to the lack of predictive skill for the Pacific\_Z500ne index. In another words,

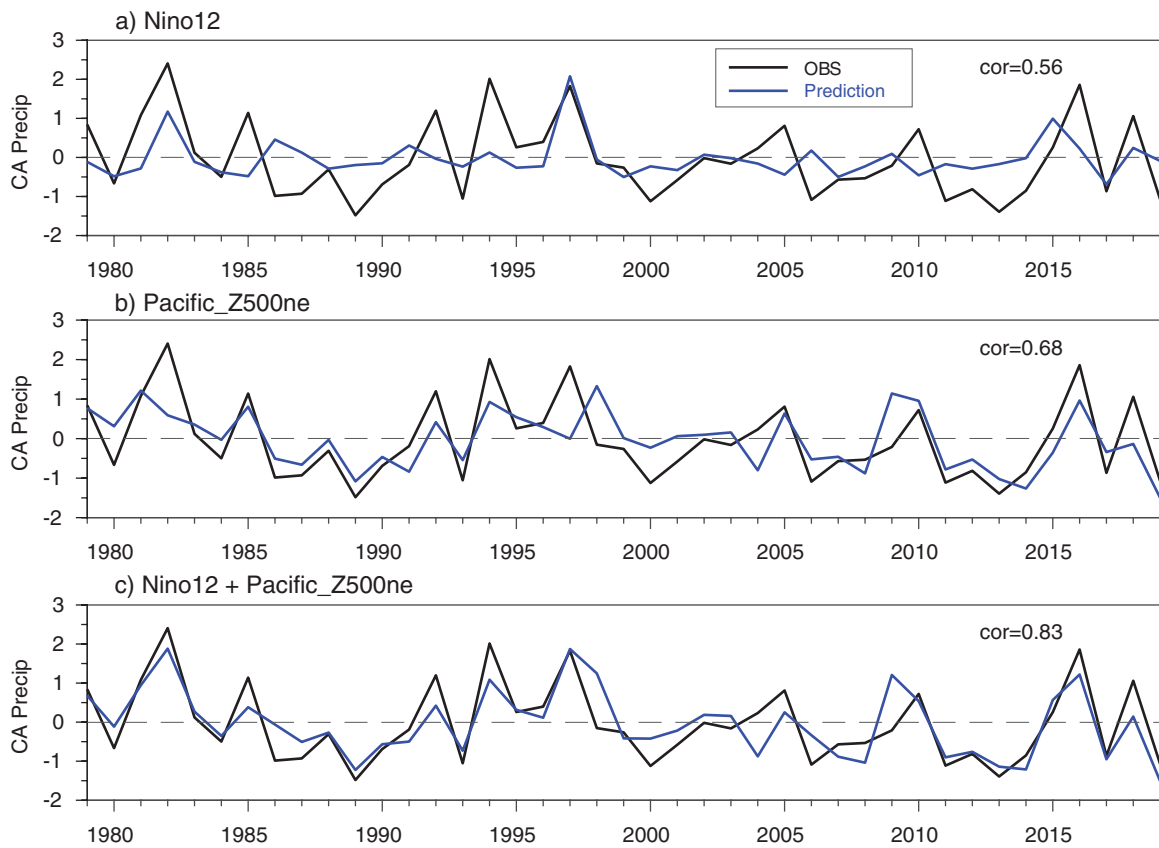


**Fig. 4.** Predicted CA winter precipitation (blue; mm day<sup>-1</sup>) based on a linear regression approach using the observed winter (a) Niño-1+2, (b) Pacific\_Z500ne, and (c) both Niño-1+2 and Pacific\_Z500ne indices, along with the observations (black).

seasonal prediction skill for CA winter precipitation is mainly relying on ENSO signals. This is further confirmed by the predicted CA precipitation based on the regression model used for Fig. 4c, but replacing the observed winter Niño-1+2 and Pacific\_Z500ne indices with the CESM1 predictions (supporting Fig. S3). For example, predictions by using both CESM1 predicted winter Niño-1+2 and Pacific\_Z500ne indices in the regression model shows a correlation of 0.34 with the observations, close to the skill directly based on CESM1 (Fig. 2a). When the CESM1 predicted Niño-1+2 index along with the observed Pacific\_Z500ne index are used, the skill score is significantly increased to 0.71. Very similar results on predictive skill of the Niño-1+2 and Pacific\_Z500ne indices are also found in other NMME models (see supporting Fig. S4 for GEOS5).

The limited skill for the Pacific\_Z500ne index in NMME models could be due to the lack of predictability of the ENSO-independent circulation anomalies as a result of strong internal atmospheric variability in the midlatitudes (e.g., Baxter and Nigam 2015; Kumar and Chen 2020), but also could be due to coupled model deficiencies in SST and associated convection anomalies beyond ENSO and/or Arctic sea ice variability that have been suggested to have some influence on circulation patterns over the west coast NA (e.g., Wang et al. 2014; Palmer 2014; Lee et al. 2015; Hartmann 2015; Cohen et al. 2017; Guan et al. 2021). To shed light on this, predictability of the Pacific\_Z500ne index is further examined by analyzing a large ensemble of Atmospheric Model Intercomparison Project (AMIP)-type climate simulations which participated in the NOAA Facility for Climate Assessments (FACTS; Murray et al. 2020). In total, 84 AGCM members from seven FACTS models (12 members from each model; see supporting Table S1 for details) are analyzed. All these individual members of AGCM simulations are forced by the same observed monthly mean SST and sea ice, which makes it possible to effectively extract the forced Pacific\_Z500ne variability in response to the observed SST

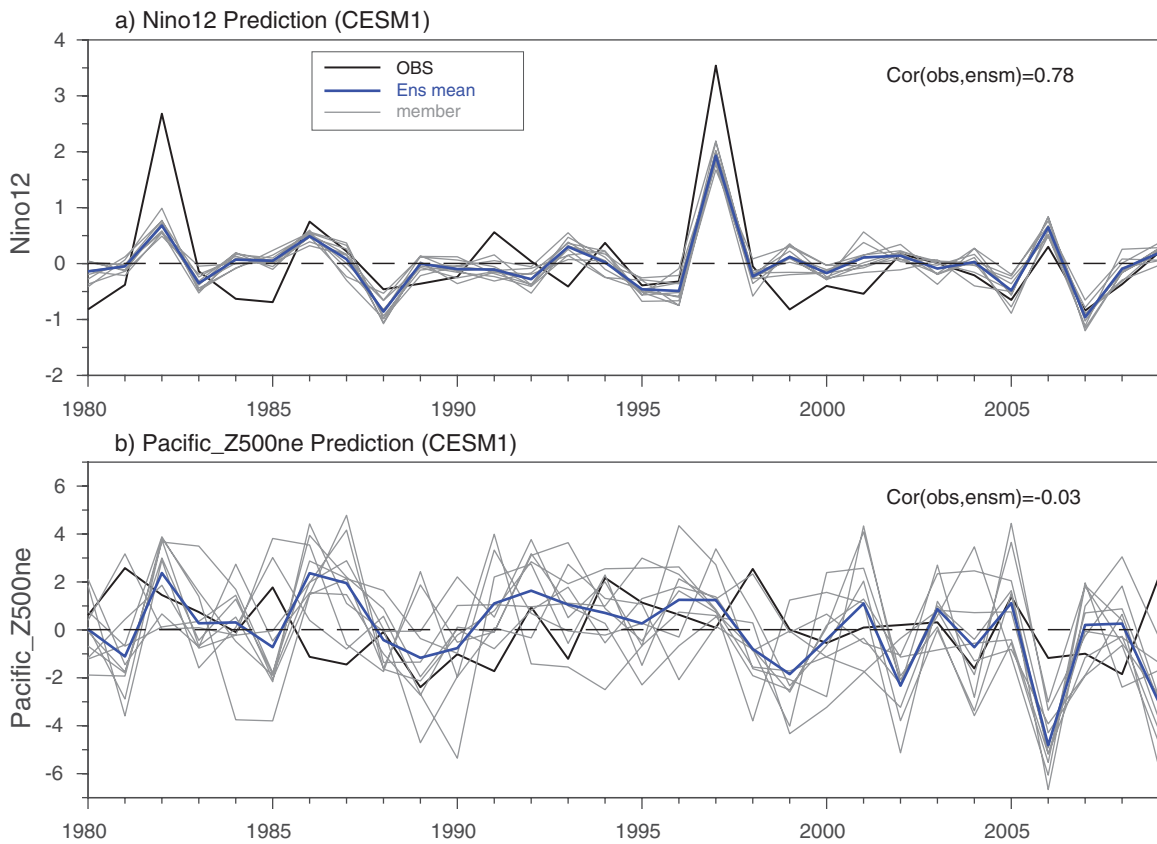


**Fig. 5.** As in Fig. 2, but for the observed (black) and predictions (blue for the multimember ensemble mean and gray for each individual member) of (a) winter Niño-1+2 and (b) Pacific\_Z500ne indices based on CESM1 hindcasts initialized on 1 Oct.

and sea ice based on the ensemble mean of simulations, in which the internal variability is significantly averaged out. Similarly, the Pacific\_Z500ne index in AGCM simulations can also be derived by projecting simulated winter mean Z500 anomalies, after removal of the ENSO component using the regression approach,<sup>3</sup> onto the observed ENSO-independent Z500 anomalies associated with CA precipitation (the red box in Fig. 3c).

<sup>3</sup> The Z500 anomalies associated with ENSO is calculated independently in each model by regressions onto the observed Niño-1+2 index.

As illustrated in Fig. 6, the 84-member averaged Pacific\_Z500ne index based on FACTS model simulations only shows a moderate correlation (~0.41) with the observations, suggesting that less than 20% of the observed Pacific\_Z500ne can be attributed to the observed

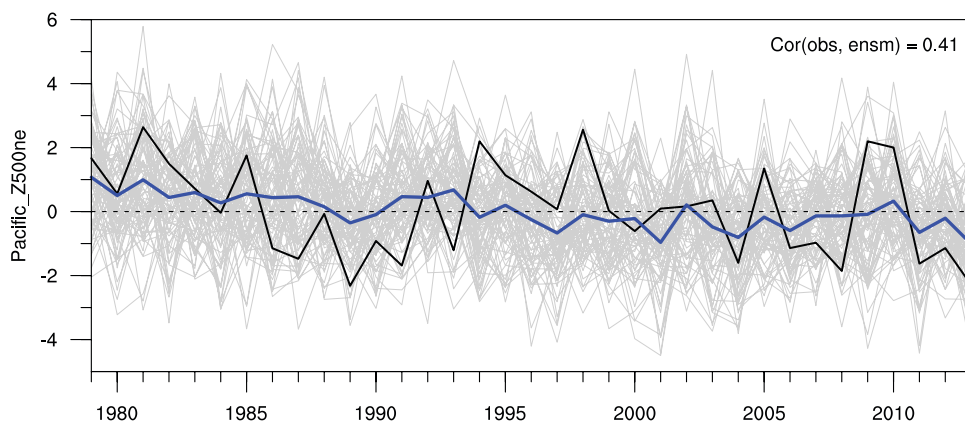


**Fig. 6.** The Pacific\_Z500ne index simulated by 84 AGCMs participated in the NOAA FACTS Project (the blue line for multimember ensemble mean, and gray by individual member simulations) along with the observations (black).

SST and sea ice variability given the atmospheric responses to SST/sea ice are perfectly represented. The low predictability in Pacific\_Z500ne by SST and sea ice is further indicated by the weak amplitude of the ensemble mean Pacific\_Z500ne while large spread among simulations from individual members.<sup>4</sup> This result suggests that the internal atmospheric variability can play a significant role in modulating the circulation anomalies over the west coast NA, which may explain poor prediction skill of the Pacific\_Z500ne index in NMME models, although there is also possibility that some predictability sources for the Pacific\_Z500ne may not be fully represented in these models due to model deficiencies. This will be further discussed.

<sup>4</sup> Amplitude of the ensemble mean Pacific\_Z500ne and their correlations to the observations vary in individual models (see supporting Fig. S5).

## Summary and discussion

Due to frequent occurrence of persistent and/or severe droughts over CA in the recent decade, there is an urgent demand for skillful seasonal prediction of CA winter precipitation for water-related disaster preparation and water management purposes. Despite the consensus that large-scale conditions, such as ENSO, exert significant influences on the year-to-year variability of CA precipitation, our predictive skill for winter mean CA precipitation remains rather limited based on both statistical and dynamical approaches. For example, when initialized in October, the state-of-the-art dynamical coupled NMME models generally only show a correlation skill of about 0.3 for CA winter prediction (see Fig. 2). In this study, we attempt to understand the key limiting factors underlying low predictive skill of CA precipitation, by focusing on predictability of the anomalous circulation pattern associated with the year-to-year variability of CA precipitation beyond the influences of the ENSO.

It is shown that only about 25% of interannual variability of CA winter precipitation can be attributed to the remote influences by tropical Pacific SST variability associated with El Niño/La Niña conditions (Fig. 1). Instead, the year-to-year CA winter precipitation variability is primarily due to circulation anomalies that are independent from ENSO, characterized by a circulation center over the west coast United States as a part of a short Rossby wave train spanning over the extratropical North Pacific (Fig. 3). Tests based on a multilinear regression model show that CA precipitation variability can be well predicted provided perfect predictions of the winter El Niño condition and the ENSO-independent circulation anomalies over the west coast United States (Fig. 4). Hindcasts based on the NMME models, however, suggest that while the winter El Niño condition can be skillfully predicted in October, these dynamical models show nearly no skill in predicting the ENSO-independent circulation anomalies (Fig. 5), leading to poor predictive skill for CA winter precipitation. Low predictability of these circulation anomalies that are independent from the ENSO variability is further demonstrated by a large number of AMIP-type AGCM simulations forced by the observed global SST and sea ice (see Fig. 6). These results suggest that less than 20% of the ENSO-independent circulation anomalies associated with CA precipitation can be explained by global SST and sea ice variability.

This study indicates that significantly improved prediction of the circulation anomalies over the west coast United States that are independent from the ENSO will be critical for any major breakthrough in predicting CA precipitation. As previously discussed, while difficulty in predicting these ENSO-independent circulation anomalies could be due to chaotic atmospheric internal processes, chances may still exist for improvement of CA precipitation prediction with possible missing predictability sources in the NMME forecast models and FACTS AGCMs. For example, as shown in Fig. 3c, while the ENSO-independent circulation anomalies associated with CA precipitation is closely linked to a wave train of short Rossby waves over the North Pacific, the formation mechanism of this wave train remains largely elusive. Noteworthy is that a similar short Rossby wave train over the North Pacific has also been observed associated with CA precipitation on the intraseasonal time scales, which tends to be further linked

to intraseasonal convective activity over the western Pacific and Indian Ocean (Teng and Branstator 2017; Siler et al. 2017; Gibson et al. 2020b, 2021). Therefore, there could exist an upscale influences on winter mean circulation anomalies associated with CA precipitation from the tropical intraseasonal variability (e.g., Peings et al. 2022). However, it has been well recognized that our current climate models have great difficulties in representing the tropical intraseasonal variability and its teleconnection to the middle to high latitudes (e.g., Stan et al. 2017; Jiang et al. 2020; Stan et al. 2022). Moreover, accurate depiction of the coupling processes between the troposphere and stratosphere, which plays crucial roles in regulating both tropical convective variability [e.g., the quasi-biennial oscillation (QBO)] and Arctic sea ice-induced mid- to high-latitude circulation anomalies, can represent another great challenge for present-day climate models (Kidston et al. 2015; Jiang et al. 2020; Kim et al. 2020), including the NMME and FACTS models analyzed in this study, due to their relatively coarse resolutions and low-top configurations. Future investigations on the formation mechanisms of the ENSO-independent circulation patterns associated with CA precipitation based on improved observations and modeling systems (e.g., the high-top global cloud permitting model) should lead to further important insights into improved understanding and prediction of CA precipitation variability.

Some caveats of this study need to be mentioned. For example, extraction of ENSO-related circulation anomalies associated with CA precipitation is based on a linear regression onto the Niño-1+2 index, which may have some limitations related to nonlinearity in the response to different phases of ENSO. Therefore, the ENSO-independent anomalies derived in this study could also contain signals associated with ENSO-related nonlinear processes, e.g., ENSO interaction with other climate variability modes. Moreover, while this study is mainly based on the period of 1979–2019, circulation patterns associated with the year-to-year variability of CA winter precipitation can also be modulated by lower-frequency climate variability modes (e.g., the Pacific decadal oscillation), the long-term climate trend, and local human activities (e.g., Yoon et al. 2015; Swain et al. 2016; Mamalakis et al. 2018; Williams et al. 2018; Swain et al. 2018; Fasullo et al. 2018; Gibson et al. 2020b). Furthermore while sensitivity testing was carried out for difference indices, the full diversity of El Niño events are difficult to capture in any single index (e.g., Paek et al. 2017; Patricola et al. 2020; Kumar and Chen 2020). Considering the need for management of water storage in a drought prone region, further investigation on precipitation predictability over various basins in California is also warranted.

**Acknowledgments.** This study was supported by California Department of Water Resources. We are grateful to Jeanine Jones and Mike Anderson for their support and guidance. We thank three anonymous reviewers for their insightful comments on an earlier version of this manuscript. XJ and GC also acknowledge partial support by NASA 80NSSC21K1522 (GC, XJ) and NOAA Climate Program Office under Award NA17OAR4310261 (XJ). The contribution of DEW was carried out on behalf of the Jet Propulsion Laboratory, California Institute of Technology, under a contract with NASA.

**Data availability statement.** CPC unified precipitation data were downloaded from [https://ftp.cpc.ncep.noaa.gov/precip/CPC\\_UNI\\_PRCP/GAUGE\\_GLB/RT/](https://ftp.cpc.ncep.noaa.gov/precip/CPC_UNI_PRCP/GAUGE_GLB/RT/). The monthly GPCP precipitation data can be assessed at [www.ncei.noaa.gov/data/global-precipitation-climatology-project-gpcp-monthly/access/](http://www.ncei.noaa.gov/data/global-precipitation-climatology-project-gpcp-monthly/access/). The ERA5 data were downloaded from the website <https://cds.climate.copernicus.eu/cdsapp#!/dataset/reanalysis-era5-pressure-levels>. The observed Niño-1+2 and Niño-3.4 indices were obtained from the NOAA Physical Science Laboratory website [https://psl.noaa.gov/gcos\\_wgsp/Timeseries/](https://psl.noaa.gov/gcos_wgsp/Timeseries/), and the ELI index was obtained from <https://portal.nersc.gov/archive/home/projects/cascade/www/ELI>. The monthly SST data from the Met Office Hadley Centre were downloaded at [www.metoffice.gov.uk/hadobs/hadisst](http://www.metoffice.gov.uk/hadobs/hadisst). The NMME model output were downloaded from [www.earthsystemgrid.org/project/nmme.html](http://www.earthsystemgrid.org/project/nmme.html). The model output from NOAA FACTS are available from [www.esrl.noaa.gov/psd/repository/alias/facts](http://www.esrl.noaa.gov/psd/repository/alias/facts).

## References

- Adler, R. F., and Coauthors, 2003: The version-2 Global Precipitation Climatology Project (GPCP) monthly precipitation analysis (1979–present). *J. Hydrometeorol.*, **4**, 1147–1167, [https://doi.org/10.1175/1525-7541\(2003\)004<1147:TVGPCP>2.0.CO;2](https://doi.org/10.1175/1525-7541(2003)004<1147:TVGPCP>2.0.CO;2).
- Barnston, A. G., and T. M. Smith, 1996: Specification and prediction of global surface temperature and precipitation from global SST using CCA. *J. Climate*, **9**, 2660–2697, [https://doi.org/10.1175/1520-0442\(1996\)009<2660:SAPOGS>2.0.CO;2](https://doi.org/10.1175/1520-0442(1996)009<2660:SAPOGS>2.0.CO;2).
- Baxter, S., and S. Nigam, 2015: Key role of the North Pacific oscillation–west Pacific pattern in generating the extreme 2013/14 North American winter. *J. Climate*, **28**, 8109–8117, <https://doi.org/10.1175/JCLI-D-14-00726.1>.
- Bayr, T., D. I. V. Domeisen, and C. Wengel, 2019: The effect of the equatorial Pacific cold SST bias on simulated ENSO teleconnections to the North Pacific and California. *Climate Dyn.*, **53**, 3771–3789, <https://doi.org/10.1007/s00382-019-04746-9>.
- Becker, E., H. van den Dool, and Q. Zhang, 2014: Predictability and forecast skill in NMME. *J. Climate*, **27**, 5891–5906, <https://doi.org/10.1175/JCLI-D-13-00597.1>.
- , B. P. Kirtman, M. L'Heureux, Á. G. Muñoz, and K. Pegion, 2022: A decade of the North American Multimodel Ensemble (NMME): Research, application, and future directions. *Bull. Amer. Meteor. Soc.*, **103**, E973–E995, <https://doi.org/10.1175/BAMS-D-20-0327.1>.
- Cash, B. A., and N. J. Burls, 2019: Predictable and unpredictable aspects of U.S. West Coast rainfall and El Niño: Understanding the 2015/16 event. *J. Climate*, **32**, 2843–2868, <https://doi.org/10.1175/JCLI-D-18-0181.1>.
- Chen, D., J. Norris, N. Goldenson, C. Thackeray, and A. Hall, 2021: A distinct atmospheric mode for California precipitation. *J. Geophys. Res. Atmos.*, **126**, e2020JD034403, <https://doi.org/10.1029/2020JD034403>.
- Chen, M., and A. Kumar, 2018: Winter 2015/16 atmospheric and precipitation anomalies over North America: El Niño response and the role of noise. *Mon. Wea. Rev.*, **146**, 909–927, <https://doi.org/10.1175/MWR-D-17-0116.1>.
- , W. Shi, P. Xie, V. B. S. Silva, V. E. Kousky, R. W. Higgins, and J. E. Janowiak, 2008: Assessing objective techniques for gauge-based analyses of global daily precipitation. *J. Geophys. Res.*, **113**, D04110, <https://doi.org/10.1029/2007JD009132>.
- Cohen, J., K. Pfeiffer, and J. Francis, 2017: Winter 2015/16: A turning point in ENSO-based seasonal forecasts. *Oceanography*, **30** (1), 82–89, <https://doi.org/10.5670/oceanog.2017.115>.
- DeFlorio, M. J., F. M. Ralph, D. Waliser, J. Jones, and M. L. Anderson, 2021: Better subseasonal-to-seasonal forecasts for water management. *Eos*, **102**, <https://doi.org/10.1029/2021E0159749>.
- Dettinger, M., 2011: Climate change, atmospheric rivers, and floods in California—A multimodel analysis of storm frequency and magnitude changes. *J. Amer. Water Resour. Assoc.*, **47**, 514–523, <https://doi.org/10.1111/j.1752-1688.2011.00546.x>.
- Fasullo, J. T., B. L. Otto-Bliesner, and S. Stevenson, 2018: ENSO's changing influence on temperature, precipitation, and wildfire in a warming climate. *Geophys. Res. Lett.*, **45**, 9216–9225, <https://doi.org/10.1029/2018GL079022>.
- Gibson, P. B., D. E. Waliser, A. Goodman, M. J. DeFlorio, L. Delle Monache, and A. Molod, 2020a: Subseasonal-to-seasonal hindcast skill assessment of ridging events related to drought over the western United States. *J. Geophys. Res. Atmos.*, **125**, e2020JD033655, <https://doi.org/10.1029/2020JD033655>.
- , ——, B. Guan, M. J. DeFlorio, F. M. Ralph, and D. L. Swain, 2020b: Ridging associated with drought across the western and southwestern United States: Characteristics, trends and predictability sources. *J. Climate*, **33**, 2485–2508, <https://doi.org/10.1175/JCLI-D-19-0439.1>.
- , W. E. Chapman, A. Altinok, L. Delle Monache, M. J. DeFlorio, and D. E. Waliser, 2021: Training machine learning models on climate model output yields skillful interpretable seasonal precipitation forecasts. *Commun. Earth Environ.*, **2**, 159, <https://doi.org/10.1038/s43247-021-00225-4>.
- Guan, W., X. Jiang, X. Ren, G. Chen, and Q. Ding, 2021: Pacific sea surface temperature anomalies as important boundary forcing in driving the interannual warm Arctic–cold continent pattern over the North American sector. *J. Climate*, **34**, 5923–5937, <https://doi.org/10.1175/JCLI-D-20-0867.1>.
- Guirguis, K., A. Gershunov, M. J. DeFlorio, T. Shulgina, L. Delle Monache, A. C. Subramanian, T. W. Corringham, and F. M. Ralph, 2020: Four atmospheric circulation regimes over the North Pacific and their relationship to California precipitation on daily to seasonal timescales. *Geophys. Res. Lett.*, **47**, e2020GL087609, <https://doi.org/10.1029/2020GL087609>.
- Hartmann, D. L., 2015: Pacific sea surface temperature and the winter of 2014. *Geophys. Res. Lett.*, **42**, 1894–1902, <https://doi.org/10.1002/2015GL063083>.
- Hersbach, H., and Coauthors, 2020: The ERA5 global reanalysis. *Quart. J. Roy. Meteor. Soc.*, **146**, 1999–2049, <https://doi.org/10.1002/qj.3803>.
- Hoell, A., M. Hoerling, J. Eischeid, K. Wolter, R. Dole, J. Perlwitz, T. Xu, and L. Cheng, 2016: Does El Niño intensity matter for California precipitation? *Geophys. Res. Lett.*, **43**, 819–825, <https://doi.org/10.1002/2015GL067102>.
- Jiang, X., and Coauthors, 2020: Fifty years of research on the Madden-Julian oscillation: Recent progress, challenges, and perspectives. *J. Geophys. Res. Atmos.*, **125**, e2019JD030911, <https://doi.org/10.1029/2019JD030911>.
- Jong, B.-T., M. Ting, and R. Seager, 2016: El Niño's impact on California precipitation: Seasonality, regionality, and El Niño intensity. *Environ. Res. Lett.*, **11**, 054021, <https://doi.org/10.1088/1748-9326/11/5/054021>.
- Kidston, J., A. A. Scaife, S. C. Hardiman, D. M. Mitchell, N. Butchart, M. P. Baldwin, and L. J. Gray, 2015: Stratospheric influence on tropospheric jet streams, storm tracks and surface weather. *Nat. Geosci.*, **8**, 433–440, <https://doi.org/10.1038/ngeo2424>.
- Kim, H., J. M. Caron, J. H. Richter, and I. R. Simpson, 2020: The lack of QBO-MJO connection in CMIP6 models. *Geophys. Res. Lett.*, **47**, e2020GL087295, <https://doi.org/10.1029/2020GL087295>.
- Kirtman, B. P., and Coauthors, 2014: The North American Multimodel Ensemble: Phase-1 seasonal-to-interannual prediction; phase-2 toward developing intraseasonal prediction. *Bull. Amer. Meteor. Soc.*, **95**, 585–601, <https://doi.org/10.1175/BAMS-D-12-00050.1>.
- Kumar, A., and M. Chen, 2020: Understanding skill of seasonal mean precipitation prediction over California during boreal winter and role of predictability limits. *J. Climate*, **33**, 6141–6163, <https://doi.org/10.1175/JCLI-D-19-0275.1>.
- Lee, M.-Y., C.-C. Hong, and H.-H. Hsu, 2015: Compounding effects of warm sea surface temperature and reduced sea ice on the extreme circulation over the extratropical North Pacific and North America during the 2013–2014 boreal winter. *Geophys. Res. Lett.*, **42**, 1612–1618, <https://doi.org/10.1002/2014GL062956>.
- L'Heureux, M. L., M. K. Tippett, and A. G. Barnston, 2015: Characterizing ENSO coupled variability and its impact on North American seasonal precipitation and temperature. *J. Climate*, **28**, 4231–4245, <https://doi.org/10.1175/JCLI-D-14-00508.1>.
- , A. F. Z. Levine, M. Newman, C. Ganter, J.-J. Luo, M. K. Tippett, and T. N. Stockdale, 2020: ENSO prediction. *El Niño Southern Oscillation in a Changing Climate*, *Geophys. Monogr.*, Vol. 253, Amer. Geophys. Union, 227–246.
- , M. K. Tippett, and E. J. Becker, 2021: Sources of subseasonal skill and predictability in wintertime California precipitation forecasts. *Wea. Forecasting*, **36**, 1815–1826, <https://doi.org/10.1175/WAF-D-21-0061.1>.
- Mamalakis, A., J.-Y. Yu, J. T. Randerson, A. AghaKouchak, and E. Foufoula-Georgiou, 2018: A new interhemispheric teleconnection increases predictability of winter precipitation in southwestern US. *Nat. Commun.*, **9**, 2332, <https://doi.org/10.1038/s41467-018-04722-7>.
- Murray, D., and Coauthors, 2020: Facility for Weather and Climate Assessments (FACTS): A community resource for assessing weather and climate variability. *Bull. Amer. Meteor. Soc.*, **101**, E1214–E1224, <https://doi.org/10.1175/BAMS-D-19-0224.1>.
- Paek, H., J.-Y. Yu, and C. Qian, 2017: Why were the 2015/2016 and 1997/1998 extreme El Niños different? *Geophys. Res. Lett.*, **44**, 1848–1856, <https://doi.org/10.1002/2016GL071515>.

- Palmer, T., 2014: Record-breaking winters and global climate change. *Science*, **344**, 803–804, <https://doi.org/10.1126/science.1255147>.
- Patricola, C. M., J. P. O'Brien, M. D. Risser, A. M. Rhoades, T. A. O'Brien, P. A. Ullrich, D. A. Stone, and W. D. Collins, 2020: Maximizing ENSO as a source of western US hydroclimate predictability. *Climate Dyn.*, **54**, 351–372, <https://doi.org/10.1007/s00382-019-05004-8>.
- Peings, Y., Y. Lim, and G. Magnusdottir, 2022: Potential predictability of south-west U.S. rainfall: Role of tropical and high-latitude variability. *J. Climate*, **35**, 1697–1717, <https://doi.org/10.1175/JCLI-D-21-0775.1>.
- Ralph, F. M., and Coauthors, 2017: Atmospheric rivers emerge as a global science and applications focus. *Bull. Amer. Meteor. Soc.*, **98**, 1969–1973, <https://doi.org/10.1175/BAMS-D-16-0262.1>.
- Rayner, N. A., D. E. Parker, E. B. Horton, C. K. Folland, L. V. Alexander, D. P. Rowell, E. C. Kent, and A. Kaplan, 2003: Global analyses of sea surface temperature, sea ice, and night marine air temperature since the late nineteenth century. *J. Geophys. Res.*, **108**, 4407, <https://doi.org/10.1029/2002JD002670>.
- Schonher, T., and S. E. Nicholson, 1989: The relationship between California rainfall and ENSO events. *J. Climate*, **2**, 1258–1269, [https://doi.org/10.1175/1520-0442\(1989\)002<1258:TRBCRA>2.0.CO;2](https://doi.org/10.1175/1520-0442(1989)002<1258:TRBCRA>2.0.CO;2).
- Seager, R., N. Naik, M. Ting, M. A. Cane, N. Harnik, and Y. Kushnir, 2010: Adjustment of the atmospheric circulation to tropical Pacific SST anomalies: Variability of transient eddy propagation in the Pacific–North America sector. *Quart. J. Roy. Meteor. Soc.*, **136**, 277–296, <https://doi.org/10.1002/qj.588>.
- , M. Hoerling, S. Schubert, H. Wang, B. Lyon, A. Kumar, J. Nakamura, and N. Henderson, 2015: Causes of the 2011–14 California drought. *J. Climate*, **28**, 6997–7024, <https://doi.org/10.1175/JCLI-D-14-00860.1>.
- Sengupta, A., and Coauthors, 2022: Advances in subseasonal to seasonal prediction relevant to water management in the western United States. *Bull. Amer. Meteor. Soc.*, **103**, E2168–E2175, <https://doi.org/10.1175/BAMS-D-22-0146.1>.
- Siler, N., Y. Kosaka, S.-P. Xie, and X. Li, 2017: Tropical ocean contributions to California's surprisingly dry El Niño of 2015/16. *J. Climate*, **30**, 10067–10079, <https://doi.org/10.1175/JCLI-D-17-0177.1>.
- Stan, C., D. M. Straus, J. S. Frederiksen, H. Lin, E. D. Maloney, and C. Schumacher, 2017: Review of tropical-extratropical teleconnections on intraseasonal time scales. *Rev. Geophys.*, **55**, 902–937, <https://doi.org/10.1002/2016RG000538>.
- , and Coauthors, 2022: Advances in the prediction of MJO teleconnections in the S2S forecast systems. *Bull. Amer. Meteor. Soc.*, **103**, E1426–E1447, <https://doi.org/10.1175/BAMS-D-21-0130.1>.
- Swain, D. L., D. E. Horton, D. Singh, and N. S. Diffenbaugh, 2016: Trends in atmospheric patterns conducive to seasonal precipitation and temperature extremes in California. *Sci. Adv.*, **2**, e1501344, <https://doi.org/10.1126/sciadv.1501344>.
- , B. Langenbrunner, J. D. Neelin, and A. Hall, 2018: Increasing precipitation volatility in twenty-first-century California. *Nat. Climate Change*, **8**, 427–433, <https://doi.org/10.1038/s41558-018-0140-y>.
- Swenson, E. T., D. M. Straus, C. E. Snide, and A. Fahad, 2019: The role of tropical heating and internal variability in the California response to the 2015/16 ENSO event. *J. Atmos. Sci.*, **76**, 3115–3128, <https://doi.org/10.1175/JAS-D-19-0064.1>.
- Teng, H., and G. Branstator, 2017: Causes of extreme ridges that induce California droughts. *J. Climate*, **30**, 1477–1492, <https://doi.org/10.1175/JCLI-D-16-0524.1>.
- Trenberth, K. E., G. W. Branstator, D. Karoly, A. Kumar, N.-C. Lau, and C. Ropelewski, 1998: Progress during TOGA in understanding and modeling global teleconnections associated with tropical sea surface temperatures. *J. Geophys. Res.*, **103**, 14 291–14 324, <https://doi.org/10.1029/97JC01444>.
- Waliser, D., and B. Guan, 2017: Extreme winds and precipitation during landfall of atmospheric rivers. *Nat. Geosci.*, **10**, 179–183, <https://doi.org/10.1038/ngeo2894>.
- Wang, S., A. Anichowski, M. K. Tippett, and A. H. Sobel, 2017: Seasonal noise versus subseasonal signal: Forecasts of California precipitation during the unusual winters of 2015–2016 and 2016–2017. *Geophys. Res. Lett.*, **44**, 9513–9520, <https://doi.org/10.1002/2017GL075052>.
- Wang, S. Y., L. Hippias, R. R. Gillies, and J.-H. Yoon, 2014: Probable causes of the abnormal ridge accompanying the 2013–2014 California drought: ENSO precursor and anthropogenic warming footprint. *Geophys. Res. Lett.*, **41**, 3220–3226, <https://doi.org/10.1002/2014GL059748>.
- Williams, A. P., P. Gentine, M. A. Moritz, D. A. Roberts, and J. T. Abatzoglou, 2018: Effect of reduced summer cloud shading on evaporative demand and wildfire in coastal Southern California. *Geophys. Res. Lett.*, **45**, 5653–5662, <https://doi.org/10.1029/2018GL077319>.
- Williams, I. N., and C. M. Patricola, 2018: Diversity of ENSO events unified by convective threshold sea surface temperature: A nonlinear ENSO index. *Geophys. Res. Lett.*, **45**, 9236–9244, <https://doi.org/10.1029/2018GL079203>.
- Yang, X., L. Jia, S. B. Kapnick, T. L. Delworth, G. A. Vecchi, R. Gudgel, S. Underwood, and F. Zeng, 2018: On the seasonal prediction of the western United States El Niño precipitation pattern during the 2015/16 winter. *Climate Dyn.*, **51**, 3765–3783, <https://doi.org/10.1007/s00382-018-4109-3>.
- Yoon, J.-H., S. Y. S. Wang, R. R. Gillies, B. Kravitz, L. Hippias, and P. J. Rasch, 2015: Increasing water cycle extremes in California and in relation to ENSO cycle under global warming. *Nat. Commun.*, **6**, 8657, <https://doi.org/10.1038/ncomms9657>.
- Zhang, W., G. Villarini, L. Slater, G. A. Vecchi, and A. A. Bradley, 2017: Improved ENSO forecasting using Bayesian updating and the North American Multimodel Ensemble (NMME). *J. Climate*, **30**, 9007–9025, <https://doi.org/10.1175/JCLI-D-17-0073.1>.